JOURNAL OF AGRICULTURAL AND FOOD CHEMISTRY
ARTICLE

J. Agric. Food Chem. 2010, 58, 2637–2642 2637
DOI:10.1021/jf902204q

Comparable Susceptibilities of Human 293 Cells and Insect Tn-5B1-4 Cells to Photoactivated α-Terthienyl†

Qingchun Huang,* Yang Liu, Taisong Zhan, Yunfei Deng, and Yuan He

Shanghai Key Laboratory of Chemical Biology, School of Pharmacy, East China University of Science and Technology, 130 Meilong Road, Shanghai 200237, People's Republic of China

The hope is that photoactive compounds acting as potential insecticides will have reduced environmental risk, but that is not necessarily the case. In an attempt to elucidate the risk by which photoactivated α-terthienyl (α-T) affects human health, the effects of exposure of human 293 cells and insect Tn-5B1-4 cells to photoactivated α-T at certain doses were characterized. Photoactivated α-T exhibited dose dependence of toxicity and time kinetics of phototoxic activation on the growth of 293 cells (EC_{50} = 6.23 μg/mL) and Tn-5B1-4 cells (EC_{50} = 3.36 μg/mL). 293 cells appeared to be anchorage-independent, inflated, and broken; Tn-5B1-4 cells showed significant necrosis. ROS productions and lipid peroxidation of 293 cells were always lower than that of Tn-5B1-4 cells in the treatments of α-T at the same dose. Moreover, photoactivated α-T caused nonselective DNA damage in 293 and Tn-5B1-4 cells at a 10 μg/mL dose and induced cell-cycle progression of 293 cells to increase apoptosis of cells and G1 arrest and decrease in S phase cell population, whereas Tn-5B1-4 cells showed S arrest accompanied by a dose-dependent decrease in G1 and G2 phase cells at a 5 μg/mL dose. These observations suggest that Tn-5B1-4 cells are more susceptible to the action of photoactivated α-T than 293 cells, but photoactivated α-T as an efficient insecticide might be a potential factor in human mutagenic progression.

KEYWORDS: Susceptibility; 293 cells; Tn-5B1-4 cells; photoactivated α-terthienyl

INTRODUCTION

Photoinsecticidal agents, because of their lower mammalian toxicity, higher insecticidal efficiency, and environmental friendliness, are becoming new tools to decrease crop losses caused by pest insects (*1*). α-Terthienyl (α-T), a secondary metabolite extracted from the root of the marigold, is a natural plant defense being developed as an effective photoactivated pesticide (*2*). Its LD_{50} value against larvae of *Aedes aegypti* was 19 μg/kg under the exposure of ultraviolet light with 300−400 nm wavelength in comparison with 62 μg/kg for malathion and 70 μg/kg for DDT at the same conditions (*3*). Even with doses of 10−100 g of active ingredient (ai)/hm^2, α-T still showed high efficiency to control larvae of *A. aegypti* and *Anopheles gambiae* in natural pools (*4*,*5*). Up to now, many terthienyl derivatives had been synthesized such as oligothiophenes, thienyl 1,3,4-thia(oxa)diazoles, and substituted α-terthienyls, and some were commercially applied as photoactive pesticides or medicines in the United States and Canada (*7*−*11*).

The photoexcitation of α-T was reported as an oxygen-dependent process; α-T was readily reduced in the metastable triplet state from the excited singlet manifold, and the electron was subsequently transferred to molecular oxygen, forming reactive superoxide anions (*1*, *10*, *12*, *13*). Many physiological studies showed that photoactivated α-T inactivated superoxide dismutase in the anal gills of *A. aegypti*, diminished tyrosinase activity, and induced the development of insect into abnormal pupae with aberrant cuticles (*14*−*16*). Efficiency optimization of terthienyl derivatives and other phototoxins on pest insects simultaneously called attention to the improvement of the ecological safety of the photosensitizers on mammals, especially their function on human internal microenvironment.

Herein, photooxidative effects of α-T, as a typical phototoxin representative, were investigated on the susceptibility of human 293 cells and insect Tn-5B1-4 cells, in vitro. The differential responses of 293 and Tn-5B1-4 cells to photoactivated α-T were displayed by the determination of their morphologic toxicity, physiological reaction, DNA stability, and the profiles of cell-cycle distribution and apoptosis. The aim was to provide experimental data at the cell level for the biorational design of novel synthetic photosensitizers with higher photoeffects on pest insects and the minimized risk toward nontarget creatures in practical uses.

MATERIALS AND METHODS

Chemicals. α-Terthienyl (α-T), trypan blue, and 2′,7′-dichlorofluorescein diacetate (DCF-DA) were purchased from Sigma-Aldrich Chemicals (Bornem, Belgium). Fetal bovine serum (FBS) was from PAA Laboratories (Pasching, Austria). Dulbecco's modified Eagle's medium (DMEM) and TNM-FH medium were from HyClone (Logan, UT). Trypsin was supplied by Gibco (Gaithersburg, MD). 2-Thiobarbituric acid (TBA), trichloroacetic acid, sodium meta-arsenite, normal melting point agarose (NMA), low melting point agarose (LMA), propidium

†Part of the ECUST-Qian Pesticide Cluster.
*Corresponding author (telephone 86-21-6425-2945-8331; fax 86-21-6425-2603; e-mail qchuang@ecust.edu.cn).

Published on Web 12/16/2009

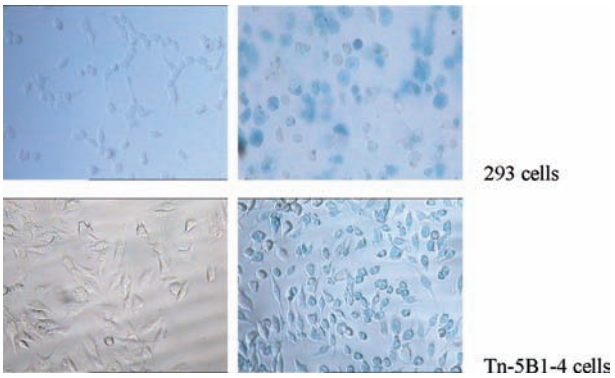

Figure 1. Cell morphology of 293 and Tn-5B1-4 cells after treatment with photoactivated α-T for 2 h. The left is dark treatment, and the right is treatment of 5 μg/mL photoactivated α-T.

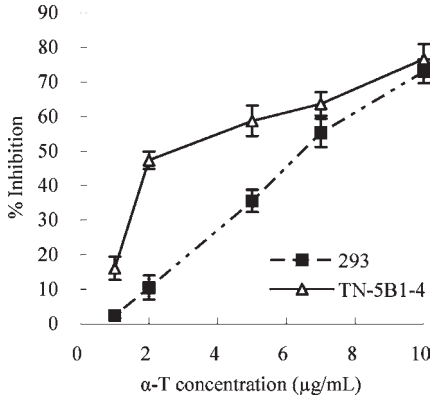

Figure 2. Average inhibition of photoactivated α-T on the viability of 293 and Tn-5B1-4 cells at 2 h post-treatment. All treatments were irradiated by only black light for 15 min.

iodide (PI), and RNase were purchased from Sinopharm Chemical Reagent Corp. (Shanghai, China).

A stock solution of α-T was dissolved in acetone with a concentration of 10.0 mg/mL and diluted in culture media to desired concentrations for experimental use.

Cell Culture. Human embryonic kidney 293 cell line was from the State Key Laboratory of Bioactivator Engineering, East China University of Science and Technology (Shanghai, China). The cells were cultured in DMEM supplemented with 10% FBS and maintained at 37 °C in a humidified incubator containing 5% CO_2 and 95% air. *Trichoplusia ni* Tn-5B1-4 cell line was from the Laboratory of Insect Molecular Biology, Zhejiang University (Hangzhou, China). The cells was cultured in TNM-FH medium supplemented with 10% FBS and maintained at 27 °C/100% air in a humidified incubator (Sanyo MCO-15AC, Japan).

α-T Exposure. Culture media of 293 and Tn-5B1-4 cells at exponentially growing stage were removed, and then the cells were washed twice with cold PBS buffer (8.00 g of NaCl, 0.20 g of KCl, 1.29 g of $Na_2HPO_4 \cdot H_2O$, 0.20 g of KH_2PO_4, 1000 mL of ddH_2O), detached by using 0.25% trypsin solution, and then suspended in 2 mL of culture medium at a density of (2.0−3.0) × 10^5 cells/mL. One hundred microliters of the single cell suspension was seeded in a 96-well plate, and the diluted solution of α-T was added to attain final concentrations of 1, 2, 5, 7, and 10 μg/mL in the medium, respectively. All treatments were irradiated to achieve maximum intensity under a black light (40 W, UV 250 mW cm^{-2}, 17 cm distance) for 15 min at room temperature. Identical treatments were placed in the dark for the same time at room temperature. After irradiation, cultures were sent back to the incubator and allowed to incubate for 2 h. All treatments were used for next determination.

Assessment of Cell Viability. Cellular viability was measured using trypan blue dye exclusion according to the method of Gutting et al. (*17*) with minor modification. Cells in all above treatments were trypsinized and resuspended in 200 μL of medium, and then 200 μL of 0.4% trypan blue solution was added. Cells were immediately examined for trypan blue uptake using a Leica DMIRB imaging system. Photographs (40×) were taken of each culture well for all treatment and untreated groups. The clear cells were alive and the blue cells were dead. α-T inhibition values, in triplicate, were expressed as percentage of untreated cells by counting individual live and dead cells in the photographs.

Measurement of Reactive Oxygen Species (ROS). Intracellular ROS of live cells were measured by fluorescent analysis of DCF-DA according to the method of Levovich et al. (*18*). In cells, the dye being deacetylated by intracellular esterases and oxidized by ROS emitted fluorescent light. Cultures in 96-well plates were exposed to photoactivated α-T as the above procedure, and then DCF-DA solution was added at a final concentration of 5 μg/mL in the medium. The treated cultures were allowed to incubate continually for 2 h. Cells were washed twice with PBS, and ROS generation of cells was examined by using a fluorescent microtiter plate photometer (Synergy2 BioTek) with a 488 nm excitation beam. The results represented the percentage of ROS production in α-T treatments relative to that in the control groups.

Measurement of Malondialdehyde (MDA) Production. The level of MDA, an end product of lipid peroxidation in cultures, was determined according to the method described by Stocks et al. (*19*). Exponentially, cells in 2 mL of culture were exposed to photoactivated α-T for 15 min, and 1.0 mL of 28% trichloroacetic acid−sodium meta-arsenite solution was added. Then, the cultures were centrifuged at 4000*g* for 10 min. The supernatants were mixed with 0.5 mL of 0.6% TBA solution and bathed in 100 °C for 15 min. After cooling, the mixture was centrifuged at 4000*g* for 10 min. The sediments were discarded, and the absorbance of supernatants was measured at 532 nm by using a fluorescent microtiter plate photometer (Synergy2 BioTek). The concentration of MDA in culture was calculated by the absorbance coefficient of the MDA−TBA complex, 1.56 × 10^5 L/mol·cm and expressed in nanomoles per liter.

Single-Cell Microgel Electrophoresis (SCGE) for DNA Damage Analysis. DNA damage of photoactivated α-T on cells was conducted using alkaline SCGE as described previously with minor modification (*20*, *21*). Ten microliters of cell suspension (1.0 × 10^6 cells/mL) was mixed with 90 μL of 0.8% LMA in Ca^{2+}- and Mg^{2+}-free PBS to form a mixture. The mixture was rapidly spread over a precleaned microscope slide (75 mm × 25 mm) previously conditioned by spreading 100 μL of 1% NMA in Ca^{2+}- and Mg^{2+}-free PBS. After solidification, the cells were protected with a top layer of 100 μL of 0.8% LMA. The slides were immersed in freshly prepared ice-cold lysis buffer (2.5 mol/L NaC1, 100 mmo1/L EDTA, 10 mmol/L Tris-HCl, 1.0% sodium lauroyl sarcosinate, pH 10, with 10% DMSO and 1.0% Triton X-100 added just before use) at 4 °C for 2 h in the dark and then placed on a horizontal electrophoresis box filled with freshly made alkaline buffer (1.0 mmo1/L EDTA, 300 mmo1/L NaOH, pH 13) to unwind DNA double strands thoroughly for 20 min. Electrophoresis was performed for 20 min at an electric field of 25 V and the current of 200 mA. After electrophoresis, the slides were neutralized in 0.4 mol/L precooled Tris-HCl buffer (pH 7.5) and stained by 0.2 mg/mL PI at 4 °C for 30 min. DNA damage was photographed under a fluorescent microscope and analyzed with Gel-Pro software. DNA mobility was expressed as the ratio of tail length divided by the diameter of the comet head; 30 cells from each of three replicate slides were analyzed for each concentration of photoactivated α-T. The results represent the percentage of DNA mobility in α-T treatments relative to that in the control groups.

Flow Cytometry Analysis for Cell-Cycle Analysis. Cell-cycle and apoptosis analysis was performed with a flow cytometer (FACSCalibur, Becton Dickinson) according to the method described by Gougeon and Montagnier (*22*). Two milliliters of 1.0 × 10^6 cells/mL cell suspension was centrifuged at 1000*g* and 4 °C for 5 min, and 2.0 × 10^6 cells were collected and washed once with cold PBS. Cells pelleted by spinning at 1000*g* and 4 °C for 5 min were resuspended in 0.6 mL of cold PBS, fixed, and permeabilized by adding 1.4 mL of absolute ethanol at −20 °C overnight. The fixed cells were centrifuged as above and washed twice with cold PBS, then lysed in 1.0 mL of 50 μg/mL RNaseA for 30 min followed by centrifugation (1000*g*, 4 °C, 5 min) and incubation with 1.0 mL of 50 μg/mL PI for 30 min in darkness at room temperature. Data acquisition and analysis were performed in the flow cytometer with the accompanying CellQuest software procedure. Plots were drafted with PI fluorescence value as *X*-axis and cell number as *Y*-axis.

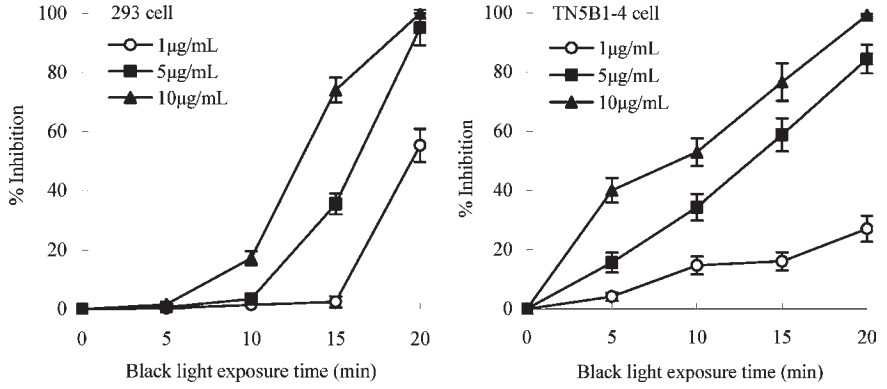

Figure 3. Effect of black light exposure time on the cell viability inhibition of α-T against 293 and Tn-5B1-4 cells. The data represent the average values from three separated experiments. All data were calculated relative to dark treatments.

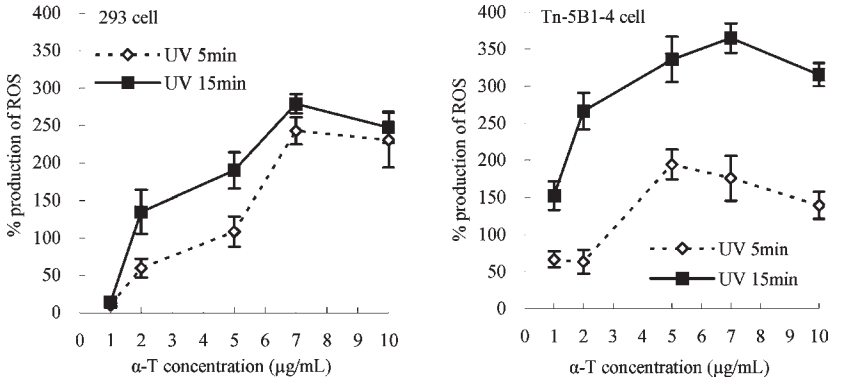

Figure 4. Intracellular ROS production of 293 and Tn-5B1-4 cells at 2 h post-treatment by photoactivated α-T with 5 and 15 min black light exposures. The values represent the mean ± SD for three independent determinations. All data were calculated relative to dark treatments.

Statistical Analysis. Each parameter was calculated and expressed as the mean ± standard deviation (SD) or the mean value of three independent experiments. Statistical analysis was carried out using the one-way analysis of variance (ANOVA) by a least significant difference (LSD) multiple-range test. A value of $p < 0.05$ or $p < 0.01$ was considered to be statistically significant.

RESULTS

Cytotoxicity of α-T. After treatment by photoactivated α-T, obvious cytotoxic morphosis was observed in all cell lines; some cells showed breakage, intracellular leakage, even death. The morphology of 293 and Tn-5B1-4 cells was photographed for **Figure 1**. In the control, 293 and Tn-5B1-4 cells exhibited high viability and good adherence; no obvious trypan blue staining emerged. In the treatments by photoactivated α-T, 293 cells appeared to be anchorage-independent, inflated, or broken and/or showed significant trypan blue staining. However, Tn-5B1-4 cells were not inflated and still anchorage-dependent, but significant cell death was observed.

Effect of Photoactivated α-T on Cell Viability. Photoactivated α-T showed significant dose-dependent toxicity on cell viability of test cell lines. As shown in **Figure 2**, a straight-line relationship between the concentrations of α-T and its percentage inhibition on cell viability was obtained in 293 cells; its corresponding EC_{50} value was 6.23 μg/mL. Tn-5B1-4 cells appeared to be more significantly susceptible to the inhibition of photoactivated α-T than 293 cells did ($P < 0.05$, ANOVA). The linear inhibition range of photoactivated α-T on the viability of Tn-5B1-4 cells was above 2 μg/mL doses, and its EC_{50} value was 3.36 μg/mL.

Effect of Black Light Exposure Time on Phototoxicity of A-T against Cell Viability. The photoactive toxicity of α-T against cell viability was positively correlated with black light exposure time in all of the treatments of the test cell lines (**Figure 3**). Compared with the inhibitory rate at 5 min of exposure, the inhibitory rates of photoactivated α-T were improved up to about 50.08 times against 293 cells and improved about 3.89 times against Tn-5B1-4 cells at 15 min of exposure. Obviously, Tn-5B1-4 cells were more sensitive to the action of photoactivated α-T than 293 cells during the 15 min black light exposure. Along with the continual black light exposure, the inhibition of photoactivated α-T was stronger, but there were hardly any differences between the inhibitions of photoactivated α-T against the two test cell lines.

Intracellular ROS Production. Photoactivated α-T also showed significant dose-dependent activities on inducing ROS production of the two test cell lines, and 15 min of black light exposure excited significantly higher ROS production of the two test cell lines than 5 min of black light exposure did (**Figure 4**). For 293 cells, 1.0 μg/mL photoactivated α-T could induce ROS production of about 10.27 and 14.40%; the maximum productions of ROS were induced by 7 μg/mL photoactivated α-T up to 242.71 and 279.06% under 5 and 15 min of black light exposure, respectively. Meanwhile, for Tn-5B1-4 cells, ROS productions were always higher than those of 293 cells under 15 min of black light exposure induced by the treatments of photoactivated α-T with certain concentration ($P < 0.05$, ANOVA).

Extracellular MDA Production. As **Figure 5** indicates, for 293 cells, photoactivated α-T could slightly increase MDA content in media, but this improvement was not significantly changed with the increasing concentrations of α-T. In the case of Tn-5B1-4 cells, MDA productions were enhanced with the increasing concentrations of photoactivated α-T; the maximum improvement of MDA content in media was the treatment of

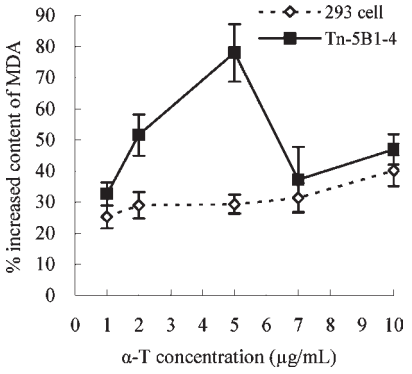

Figure 5. Content changes of MDA in the culture media of 293 and Tn-5B1-4 cells at 2 h post-treatment by photoactivated α-T with 15 min black light exposure. The values represent the mean ± SD for three independent determinations. All data were calculated relative to dark treatments.

5.0 μg/mL photoactivated α-T. However, there were no differences between MDA increased content of Tn-5B1-4 and 293 cells in the treatment of photoactivated α-T at 7.0 and 10.0 μg/mL doses.

DNA Damage Caused by Photoactivated α-T. Photoactivated α-T induced a high degree of DNA damage of 293 and Tn-5B1-4 cells, particularly in the case of 10 μg/mL α-T treatment. After 15 min of black light exposure, a significant increase of tail length and tail intensity was measured. **Figure 6A** shows the comet appearance of 293 and Tn-5B1-4 cell electrophoresis. In the control, comet heads were concentrated with high-density DNA, accompanied with smooth margin and unrecognized tail. In the treatments, comets were observed with broom-shaped tails composed by many DNA fragments, and fluorescence intensity of the tails was obviously weaker than that of the head. In particular, the comet head of 293 cells also showed significantly weaker fluorescence intensity than that of Tn-5B1-4 cells with the treatment of 10 μg/mL α-T, indicating that a higher degree of DNA strand breakage in 293 cells was induced by photoactivated α-T than in Tn-5B1-4 cells. DNA mobility was calculated and listed in **Figure 6B**. No significant difference of DNA mobility was observed between 293 and Tn-5B1-4 cells in the presence of photoactivated α-T ($P < 0.05$, ANOVA).

Cell-Cycle Protocols Induced by Photoactivated α-T. To examine the mechanism of antiproliferative activity of photoactivated α-T, cell-cycle distribution was determined by flow cytometry (**Figure 7A**). After α-T treatment with 15 min of black light exposure and continual incubation for 4 h in darkness, 293 cells displayed G1 arrest that was accompanied by a decrease in the S phase cell population; the apoptotic 293 cells dramatically increased to a level of 13.31% of counted cells with treatment of 5 μg/mL photoactivated α-T as compared to 2.30% of control cells (**Figure 7B**). In the case of Tn-5B1-4 cells, the effect of photoactivated α-T on S arrest was largely accompanied by a dose-dependent decrease in the G1 and G2 phase cells, whereas Tn-5B1-4 cells showed little apoptosis after exposure to photoactivated α-T; 16.80% of apoptotic cells at the 5 μg/mL dose was not significantly different as compared to 11.49% in the control ($P < 0.05$, ANOVA).

DISCUSSION

Although many agrochemicals have been developed and used, the side effects and resistance are serious problems that have to be overcome with the treatment of pest insects (*23*). Of particular importance are chronic sublethal effects, which in most cases are not assessed sufficiently before the introduction of new chemicals

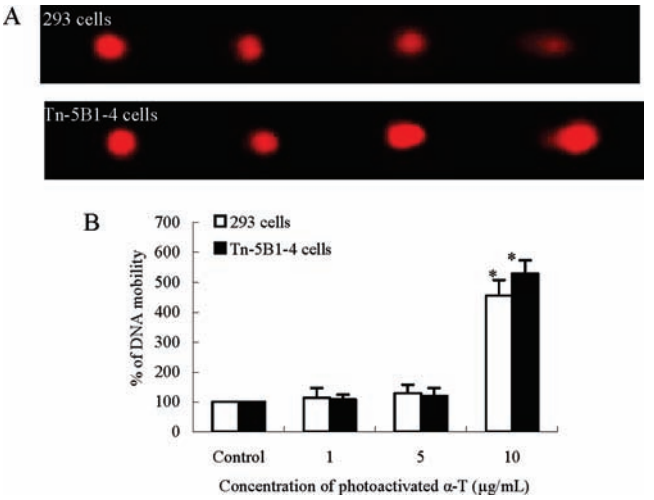

Figure 6. Single-cell microgel electrophoresis of 293 and Tn-5B1-4 cells after treatment with photoactivated α-T with 15 min black light exposure at 2 h post-treatment: (**A**) photographs of DNA comet of 293 and Tn-5B1-4 cells (concentrations of α-T from left to right were 0 (control), 1, 5, and 10 μg/mL, respectively); (**B**) quantitative assessment of DNA mobility (%) of 293 and Tn-5B1-4 cells relative to dark treatments, as treated by photoactivated α-T and representing the average of three independent experiments ± SD. ∗, $P < 0.05$.

into the environment. Photoinsecticidal agents are characterized by the use of light irradiation and oxygenous oxidization; the molecular mechanism on insects of photoinsecticidal agents is the photodynamic action of ROS such as generating singlet oxygen, superoxide anion radical, and photosensitizer radicals via type I and type II photodynamic processes (*13*, *16*, *24*, *25*). Ben Amor et al. and Heitz demonstrated that many photosensitizers such as xanthene dyes, phloxine B, and α-T had been most extensively studied as insecticides (*1*, *5*).

The present study elucidates the interspecies specificity of photoactivated α-T, a well-known photoinsecticide extracted from the root of the marigold as a typical photosensitizer, in human 293 cells and insect Tn-5B1-4 cells. The results clearly demonstrate that photoactivated α-T induced 293 cells to be anchorage-independent and inflated, but Tn-5B1-4 cells were still anchorage-dependent and not inflated. The growth of 293 cells with EC_{50} value of 6.23 μg/mL was less sensitive to the inhibition of α-T during a 15 min black light exposure than that of Tn-5B1-4 cells with EC_{50} value of 3.36 μg/mL. ROS productions of Tn-5B1-4 cells were always higher than that of 293 cells with the increasing concentrations of α-T at 15 min of black light exposure, and lipid peroxidation of Tn-5B1-4 cells was also heavier than that of 293 cells in the treatment of α-T at least at a 7 μg/mL dose. The obtained data coherently confirmed the facts about higher susceptibility of insect Tn-5B1-4 cells to photoactivated α-T compared with human 293 cells. Aplin et al. and Johansson reported that cell surface adhesion molecules (CAM), such as the immunoglobulin superfamily, the integrins, the cadherins, and the selectins, played an important role in cellular immune response processes against exogenous intoxicants (*26*, *27*). Tipton et al. and Plopper showed that extracellular matrix (ECM), an interlocking mesh of fibrous proteins and glycosaminoglycans, was involved in the cell-defending progress to exogenous drugs (*28*, *29*). The ROS generation as reported could result in significant damage on cell structures such as DNA and lipid and induce enzyme inhibition such as superoxide dismutase (*14*, *30*, *31*). It is reasonable to postulate that the differential susceptibilities to the action of photoactivated α-T might be

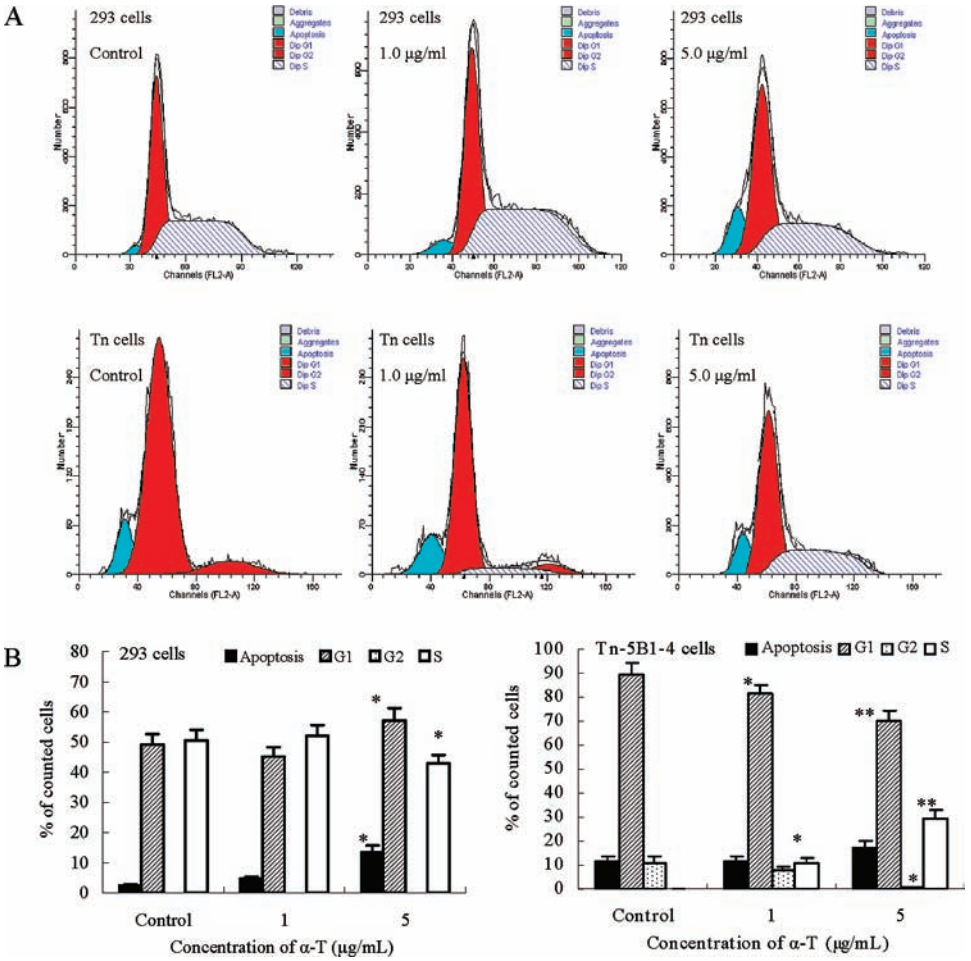

Figure 7. Cell-cycle patterns and apoptosis effects of photoactivated α-T on 293 and Tn-5B1-4 cells: (**A**) cells were treated with 0 (control), 1, and 5 μg/mL of α-T with 15 min black light exposure at 4 h post-treatment and subjected to flow cytometric analysis after PI staining; (**B**) quantitative assessment of the percentage of 293 and Tn-5B1-4 cells in cell-cycle patterns (apoptosis, G1, S, and G2 phase), as treated by photoactivated α-T and representing the average of three independent experiments ± SD. ∗, $P < 0.05$; ∗∗, $P < 0.05$.

related to the differences of CAM structure, ECM production, and antioxidant physiological systems in 293 and Tn-5B1-4 cells.

Cell-cycle progression initiates cell division by the binding of cyclin with cyclin-dependent kinases (*32*); apoptosis from S phase toward later mitosis that disciplinarily controls self-cell death plays a critical role in maintaining normal tissue homeostasis (*33*). The disturbing balance between cell proliferation and cell death inevitably leads to the development of various diseases, even individual death of pest insects (*34*, *35*). In this study, photoactivated α-T, indeed, exhibited dose dependence of toxicity and time kinetics of phototoxic activation on the growth of 293 and Tn-5B1-4 cells. 293 cells exhibited breakage and significant trypan blue staining, whereas Tn-5B1-4 cells were mostly dead. Photoactivated α-T induced nonselectively DNA damage in 293 and Tn-5B1-4 cells at 10 μg/mL dose and selectively induced apoptosis in 293 cells and death in Tn-5B1-4 cells. The increase of apoptotic cells and G1 arrest and the decrease in the S phase cell population and DNA damage in 293 cells suggest that photoactivated α-T in the human body is potentially one of the factors in mutagenic progression. A lack of apoptotic effect of photoactivated α-T in Tn-5B1-4 cells suggests that the pathways contributing to the growth inhibitory responses in insect cell type are somewhat different from that in human 293 cells.

In conclusion, photoactivated α-T, an efficient photoinsecticidal agent, presents a perfect alternative to traditional pesticides for the control of the population of pest insects. An efficacy of photoactivated α-T in the inhibition of cell growth and these mechanistic observations revealed that the growth and the antioxidant tolerance of Tn-5B1-4 cells were more susceptible to the action of photoactivated α-T than 293 cells. Photoactivated α-T may induce the apoptosis of 293 cells but promote the death of Tn-5B1-4 cells. Cell-cycle progression was regulated and significant DNA strand breakage was developed in 293 cells in the treatments of photoactivated α-T at certain doses. However, more studies are necessary to clarify the mechanism of photoactivated α-T or its derivatives. Rational uses of α-T in the field may be notified to minimize its environmental risks and decrease its significant bioaccumulation in nontarget species. Moreover, the new photoinsecticides should be designed and developed with careful modified structure that enhances the photoinsecticides to exhibit the optimized efficiency of the cytocidal effects and the environmental friendship.

ABRREVIATIONS USED

α-T, α-terthienyl; ROS, reactive oxygen species; MDA, malondialdehyde; DCF-DA, 2′,7′-dichlorofluorescein diacetate; FBS, fetal bovine serum; DMEM, Dulbecco's modified Eagle's medium; NMA, normal melting point agarose; LMA, low melting point agarose; PI, propidium iodide; CAM, adhesion molecules; ECM, extracellular matrix; SCGE, single-cell microgel electrophoresis.

LITERATURE CITED

(1) Ben Amor, T.; Jori, G. Sunlight-activated insecticides historical background and mechanisms of the phototoxic activity. *Insect Biochem. Mol. Biol.* **2000**, *30*, 915–925.

(2) Jiang, Z.; Shang, Z.; Wan, S.; Xu, H.; Chiu, S. Development and application of photoactivated pesticides. *Chinese J. Pestic. Sci.* **2001**, *3*, 1–5.

(3) Heitz, J. R.; Downum, K. R. *Light-Activated Pesticides Control*; ACS Symposium Series; American Chemical Society: Washington, DC, 1995; pp 443.

(4) Philogene, B. R. J.; Arnason, J. T.; Berg, C. W.; Duval, F.; Morand, P. Efficacy of the plant phototoxin α-terthienyl against *Aedes intrudens* and effects on non-target organisms. *J. Chem. Ecol.* **1985**, *12*, 893–898.

(5) Heitz, J. R. The development of photoactivated compounds as pesticides. In *Light-aActivated Pesticides*; ACS Sympsoium Series 339; Heitz, J., Downum, K. R., Eds.; American Chemical Society: Washington, DC, 1987; pp 1−21.

(6) Morand, P.; Arnson, J. T.; Bernard, J. R.; Philogene, G.; Anita, M. M.; Leonard, C. L.; Kaminski, J. G. Phototoxic compounds for use as insect control agents. U.S. Patent 5045563, 1991.

(7) Arnson, J. T.; Bernard, J. R.; Philogene, G. Thiophene compounds. U.S. Patent 4937256, 1995.

(8) Bernard, J. R.; Kaminski, J. G. Method of and a device for preventing the attack by oxygen-consuming organisms or parts of synthetic and natural organic materials present in the soil. CA1028945, 1996.

(9) Huang, Q.; Liu, L.; Xiao, C.; Xu, Y.; Qian, X. Photolarvicidal effect of thienyl 1,3,4-thi(ox)adiazoles and their potential DNA photocleavage. *Pestic. Biochem. Physiol.* **2004**, *79*, 42–48.

(10) Janssen, R. A. J.; Moses, D.; Sariciftci, N. S. Electron and energy transfer processes of photoexcited oligothiophenes onto tetracyanoethylene and C_{60}. *J. Chem. Phys.* **1994**, *101* (11), 9519–9527.

(11) Veith, G. D.; Mekenyan, O. G.; Ankley, G. T.; Call, D. J. QSAR evaluation of α-terthienyl phototoxicity. *Environ. Sci. Technol.* **1995**, *29*, 1267–1272.

(12) Guedes, R. C.; Eriksson, L. A. Photophysics, photochemistry, and reactivity: molecular aspects of perylenequinone reactions. *Photochem. Photobiol. Sci.* **2007**, *6*, 1089–1096.

(13) Nivsarkar, M.; Kumar, P.; Laloraya, M.; Laloraya, M. M. Generation of superoxide anion radical by α-terthienyl in the anal gills of mosquito larvae *Aedes aegypti*: a new aspect in α-terthienyl phototoxicity. *Arch. Insect Biochem. Physiol.* **1992**, *19*, 261–270.

(14) Nivsarkar, M.; Kumar, G. P.; Laloraya, M.; Laloraya, M. M. Superoxide dismutase in the anal gills of the mosquito larvae of *Aedes aegypti*: its inhibition by α-terthienyl. *Arch. Insect Biochem. Physiol.* **1991**, *16*, 249–255.

(15) Downum, K. R.; Rodriguez, E.; Towers, G. H. N. Phototoxicity to the allelochemical, α-terthienyl, to larvae of *Manduca sexta*. *Pestic. Biochem. Physiol.* **1984**, *22*, 104–109.

(16) Heitz, J. R. Pesticidal applications of photoactivated molecules. In *Light-Activated Pest Control*; Heitz, J. R., Downum, K. R., Eds.; American Chemical Society: Washington, DC, 1995; pp 1−16.

(17) Gutting, B. W.; Gaske, K. S.; Schilling, A. S.; Slaterbeck, A. F.; Sobota, L.; Mackie, R. S.; Buhr, T. L. Differential susceptibility of macrophage cell lines to *Bacillus anthracis*−Vollum 1B. *Toxicology in Vitro* **2005**, *19*, 221–229.

(18) Levovich, I.; Nudelman, A.; Berkovitch, G.; Swift, L. P.; Cutts, S. M.; Phillips, D. R.; Rephaeli, A. Formaldehyde-releasing prodrugs specifically affect cancer cells by depletion of intracellular glutathione and augmentation of reactive oxygen species. *Cancer Chemother. Pharmacol.* **2008**, *62*, 471–482.

(19) Stocks, J.; Kemp, M.; Dormandy, T. L. Increased susceptibility of red-blood-cell lipids to autooxidation in haemolytic states. *Lancet* **1971**, *7693*, 266–269.

(20) Tice, R. R.; Agurelle, E.; Anderson, D.; Burlinson, B.; Hartmann, A.; Kobayashi, H.; Miyamae, Y.; Rojas, E.; Ryu, J. C.; Sasaki, Y. F. Single cell gel/comet assay: guidelines for *in vitro* and *in vivo* genetic toxicology testing. *Environ. Mol. Mutagen.* **2000**, *35* (3), 206–221.

(21) Gabbianelli, R.; Moretti, M.; Carpenè, E.; Falcioni, G. Effect of different organotins on DNA of mollusk (*Scapharca inaequivalvis*) erythrocytes assessed by the comet assay. *Sci. Total Environ.* **2006**, *367*, 163–169.

(22) Gougeon, M. L.; Montagnier, L. Apoptosis in AIDS. *Science* **1993**, *260*, 1269–1270.

(23) Tang, Z. H.; Wu, S. X. *Genetics and Development of Insect Resistance*; Shanghai Scientific and Technological Literature Press: Shanghai, China, 2000.

(24) Bakker, J.; Gommers, F. J.; Nieuwenhius, I.; Wyenberg, H. Photoactivation of the nematicidal compound α-terthienyl from roots of marigolds (*Tagetes* species), a possible singlet oxygen role. *J. Biol. Chem.* **1979**, *254*, 1841–1844.

(25) Nivsarkar, M. Identification of α-terthienyl radical *in vitro*: a new aspect in α-terthienyl phototoxicity. *Curr. Sci.* **1999**, *76*, 1391–1393.

(26) Aplin, A. E.; Howe, A.; Alihari, S. K.; Juliano, R. L. Signal transduction and signal modulation by cell adhesion receptors: the role of integrins, cadherins, immunoglobulin-cell adhesion molecules, and selections. *Pharmacol. Rev.* **1998**, *50*, 197–263.

(27) Johansson, M. W. Cell adhesion molecules in invertebrate immunity. *Dev. Comp. Immunol.* **1999**, *23*, 303–315.

(28) Tipton, D. A.; Dabbous, M. K. Effects of nicotine on proliferation and extracellular matrix production of human gingival fibroblasts *in vitro*. *J. Periodontol.* **1995**, *66*, 1056–1064.

(29) Plopper, G. The extracellular matrix and cell adhesion. In *Cells*; Lewin, B., Cassimeris, L., Lingappa, V., Plopper, G., Eds.; Jones and Bartlett: Sudbury, MA, 2007.

(30) Yamamoto, E.; Wat, C. K.; MacRae, W. D.; Towers, G. H. N. Photoinactivation of human erythrocyte enzymes by α-terthienyl and phenylheptatriyne, naturally occurring compounds in the Asteraceae. *FEBS Lett.* **1979**, *107*, 134–136.

(31) Morallo-Rejesus, B.; Decena, A.; Phillip, J. The activity, isolation, purification and identification of the insecticidal principles from *Tagetes*. *Crop Sci.* **1983**, *7*, 31–36.

(32) Resnitzky, D.; Reed, S. I. Different roles for cyclins D1 and E in regulation of the G1-to-S transition. *Mol. Cell. Biol.* **1995**, *15*, 3463–3469.

(33) Edinger, A. L.; Thompson, C. B. Death by design: apoptosis, necrosis and autophagy. *Curr. Opin. Cell Biol.* **2004**, *l6*, 663–669.

(34) Mohan, M.; Taneja, T. K.; Sahdev, S.; Mohareer, K.; Begum, R.; Athar, R.; Sah, N. K.; Hasnain, S. E. Antioxidants prevent UV-induced apoptosis by inhibiting mitochondrial cytochrome c release and caspase activation in *Spodoptera frugiperda* (Sf9) cells. *Cell Biol. Int.* **2003**, *27*, 483–490.

(35) Budihardjo, I.; Oliver, H.; Lutter, M.; Luo, X.; Wang, X. Biochemical pathways of caspase activation during apoptosis. *Annu. Rev. Cell Biol.* **1999**, *15*, 269–290.

Received for review June 28, 2009. Revised manuscript received September 3, 2009. Accepted November 19, 2009. This work was supported by the National Key Project for Basic Research (2003CB114400) and the National Natural Science Foundation of China (30400295).